1984

Computer Modeling for Performance Analysis of Rotary Screw Compressor

M. Fujiwara

K. Kasuya

T. Matsunaga

M. Watanabe

COMPUTER MODELING FOR PERFORMANCE ANALYSIS OF ROTARY SCREW COMPRESSOR

Mitsuru Fujiwara and Katsuhiko Kasuya
Mechanical Engineering Research Laboratory, Hitachi, Ltd., Ibaraki, Japan

Tetsuzo Matsunaga
Central Research Laboratory, Hitachi, Ltd., Tokyo, Japan

Makoto Watanabe
Production Engineering Research Laboratory, Hitachi, Ltd., Kanagawa, Japan

ABSTRACT

A computer model for calculating screw compressor performance is presented. Geometrical characteristics such as volume curve, sealing line length, discharge port area, etc. are studied. The volume curve is obtained from the sealing line shape, using the principle of virtual work. This procedure has the advantage of simplifying the numerical calculation of the volume curve. An analytical model of an oil-injected screw compressor is developed, based on the laws of thermodynamics for perfect gases. The effects of internal leakage, heat exchange between gas and oil, and flow resistance at suction and discharge ports are included in the model. Some numerical examples of the P-V diagram, volumetric efficiency and adiabatic efficiency for sample rotors are demonstrated for various leakage areas and rotor wrap angles.

INTRODUCTION

Working space in a screw compressor is so complex that it is extremely difficult to analytically estimate compressor performance. However, experimental analyses are often avoided because they are expensive and special cutting tools must be rearranged for every change in rotor geometry. In addition, interlobe clearance, which exerts a significant influence on the compressor performance, is hardly kept constant throughout all types of test rotors.

Therefore, computer simulation appears to be a suitable tool for analysis of screw compressor performance. The authors previously developed a computer simulation program for a screw compressor and presented it with numerical examples[1]. However, it was applicable only to oil-free compressors and did not include the effects of discharge loss and leakage through the rotor end clearance.

The purpose of this paper is to develop a more sophisticated simulation model for analyzing oil-injected screw compressor performance, considering the presence of oil which exerts sealing and cooling effects on the compression cycle. Geometrical characteristics of rotors must be calculated before beginning the simulation and it is desirable that the calculation procedure is applicable to genaral types of rotors and as effective as possible. This is achieved by introducing new methods. For example, volume curve calculation is simplified by a unique technique using the principle of virtual work.

The present simulation program is suitable for investigating effect of rotor geometry and operating conditions on compressor performance. Numerical examples are given in cases of sample rotors having differing wrap angles.

NOMENCLATURE

A_B, A_D=blow hole area and discharge port area
A_{th}=theoretical indicated area of P-V diagram for actually discharged gas
A_i=indicated area of P-V diagram
C_p, C_v=specific heats at constant pressure and at constant volume
C_ℓ=specific heat of oil
D_M, D_F=outer diameters of male and female rotors
h=heat transfer coefficient
L_R=rotor length
ℓ_R=interlobe sealing line length
M=mass within a working space
M_{gA}=mass of gas entering from outside the system during the suction process
M_0=mass of theoretical intake gas
M_X, M_Y=geometrical moment of projected surface area on the X- and Y- planes
m=mass flow rate
N=revolutions per minute of male rotor
p=pressure
p_i=upper pressure beyond leakage path
p_A=inlet pressure
p_D=discharge pressure
q=volume flow rate
R=gas constant
R_m=apparent gas constant of gas and oil mixture
S=heat transfer area
s=center-to-center distance between the rotor axes
T=temperature
Tq=torque
Tq_i=indicated torque
t=time
V=volume
V_{gA}=volume of actual intake gas
V_0=volume of theoretical intake gas
V_{100}=volume defined by Eq.(8)

x, y, z=rectangular cordinates illustrated in Fig.1
Z=tooth number
α_1=driving rotor turning angle
α_M=male rotor turning angle
α_J=male rotor turning angle when oil injection starts
β=apparent ratio of specific heat
ε=clearance
η_{ad}, η_v=adiabatic efficiency and volumetric efficiency
κ=specific heat ratio
π_i=built-in pressure ratio
φ_M=wrap angle of male rotor
ϕ=mass ratio of oil to gas

Subscripts

BL,BT=leading blow hole and trailing blow hole
C,E=lobe tip clearance and lobe end clearance
ES=lobe end clearance leading to shaft bore
EL=lobe end clearance leading to preceding adjacent groove
ET=lobe end clearance leading to following adjacent groove
F,M=female rotor and male rotor
g, ℓ=gas and oil in working space
gi,go=gas entering and leaving working space
$\ell i, \ell o$=oil entering and leaving working space
R=interlobe clealance
1,2=driving rotor and driven rotor

GEOMETRICAL CHARACTERISTICS

Geometrical characteristics must be calculated before simulating a compression cycle, but since the construction and principles of screw compressors are described in many other papers [2], the details are omitted here.

Volume Curve

Volume curve is calculated by the following new method. Fig.1 shows meshing screw rotors. They rotate in a tight casing which is not represented in the figure. Each working space comprises a pair of grooves of male and female rotors, as illustrated by the shaded area in the figure. Compressed gas occupies the space in the grooves between the rotors and exerts rotational torque on the rotors. To calculate the amount of torque, the groove surfaces are projected to the X- and Y- planes, which are parallel to the axes of rotation of the rotors and intersect each other perpendicularly. Crosshatched areas S_1 and S_2 in Fig.1 represent the male rotor surface projections.
Fig.2 shows the projected surface of a male rotor groove on the X-plane. The contour comprises sealing lines which represent the boundary lines between the grooves, as listed in Table.1. When the meshing rotors rotate, the contour of the projected suface moves parallel to the rotor axis and does not change in the shape, as illustrated in Fig.3. It is easy to extraporate the sealing line contour beyond the rotor, as shown by the dotted lines. A geometrical moment of area about the z-axis on the X-plane is represented by:

$$M_{X1}=\int_0^{L_R} \frac{1}{2} y^2 dz \tag{1}$$

The second subscript 1 of M_{X1} refers to a given driving rotor. Similarly, M_{Y1} is defined by the following integration about the projected figure on the Y-plane.

$$M_{Y1}=\int_0^{L_R} \frac{1}{2} x^2 dz \tag{2}$$

When M_{X2} and M_{Y2} are defined in a similar manner about the driven rotor groove surface, rotational torque acting on the driving rotor caused by the gas pressure is expressed by the following equation.

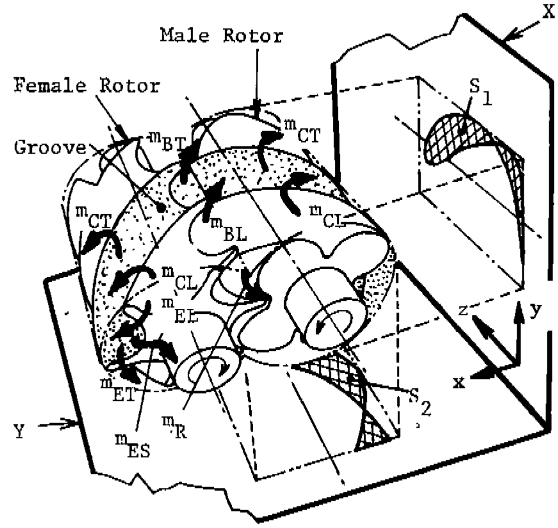

Fig.1 Screw Rotors

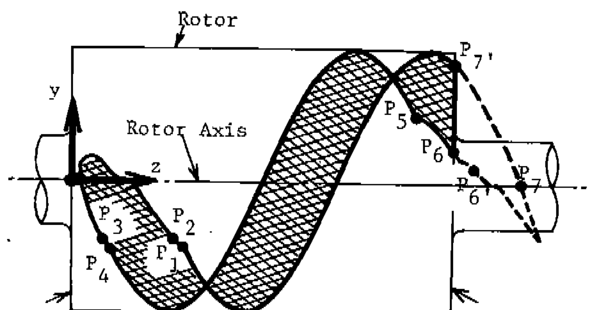

Fig.2 Projected Area of the Male Rotor on the X-Plane

Table 1 Components of Sealing Line

Section	Name	Subscript
P1-P2	Leading blow hole	BL
P2-P3	Trailing interlobe sealing line	R
P3-P4	Trailing blow hole	BT
P4-P5	Trailing lobe tip sealing line	CT
P5-P6	Blow hole on expansion side	BE
P6-P7	Leading interlobe sealing line	R
P7-P1	Leading lobe tip sealing line	CL
P6'-P7'	Lobe end sealing line	E,EL,ET

$$T_q = pM_T \tag{3}$$

where,

$$M_T = (M_{X1}+M_{Y1}) + \frac{Z_1}{Z_2}(M_{X2}+M_{Y2}) \tag{4}$$

The work done by the infinitesimal rotation of the driven rotor on the system, is equal to the product of the pressure and the change in the volume dV, and can be written as:

$$T_q d\alpha_1 = -pdV \tag{5}$$

From eq.(3) and eq.(5), the following equation is derived.

$$-pdV = pM_T d\alpha_1 \tag{6}$$

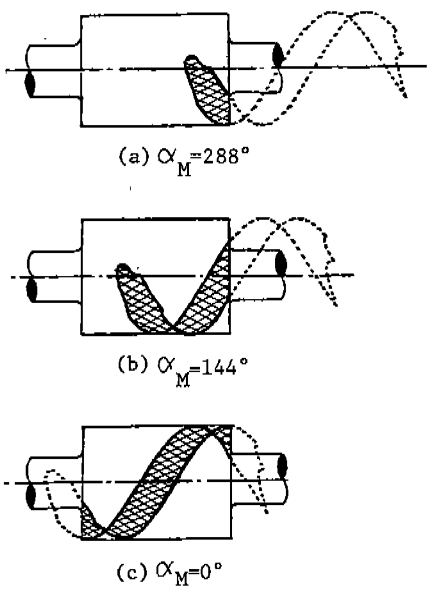

Fig.3 Movement of Sealing Line

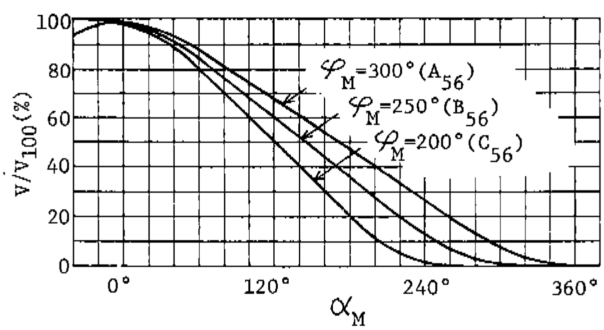

Fig.4 Volume Curves

Table 2 Sample Rotors

Name	Z_M	Z_F	D_M (mm)	D_F (mm)	S (mm)	φ_M
A_{56}	5	6	102.9	82.3	75.5	300°
B_{56}	5	6	102.9	82.3	75.5	250°
C_{56}	5	6	102.9	82.3	75.5	200°

Therefore, the following relation is obtained between volume and geometrical moment of area.

$$V = -\int_{\alpha_{10}}^{\alpha_1} M_T d\alpha_1 \tag{7}$$

where, α_{10} is the driving rotor turning angle when the volume is zero

Since the contour of the projected sealing line does not change in shape when the rotors rotate, the above relation greatly simplifies the numerical calculation of the volume curve. Fig.4 shows volume curves calculated using the above method for three sample rotors characterized on Table 2. These rotors have the same profile as illustrated in Fig.5. The origin of rotor turning angle is defined as shown in Fig.6 which represents the rotor profiles at the inlet end of the rotors. V_{100} in the ordinate is a volume defined by

$$V_{100} = (A_M + A_F)L_R \tag{8}$$

It is evident that the slope of the volume curve in Fig.4 decreases as the wrap angle increases, so, it is expected that the flow resistance at inlet and discharge ports will be small given a large wrap angle. It is also evident that the smaller the wrap angle, the larger the pressure difference across adjacent grooves, since the number of lobes, which

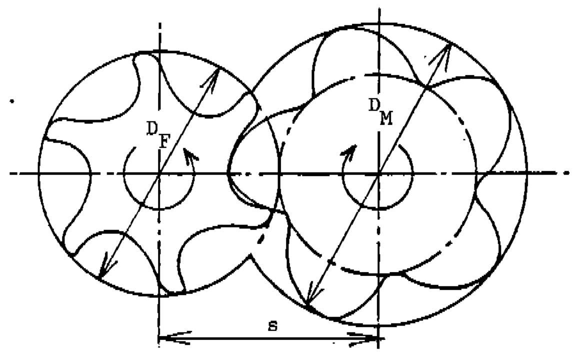

Fig.5 Profile of the Sample Rotors

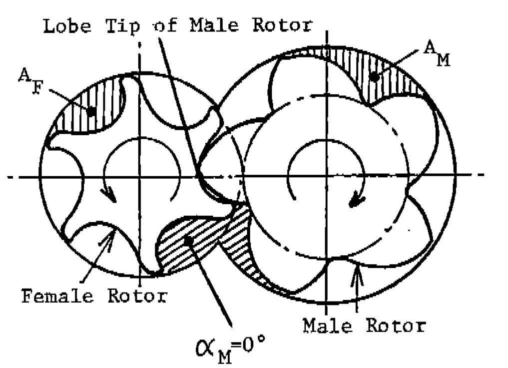

Fig.6 Origin of Rotor Turning Angle and Difinition of A_M and A_F

is directly related to the pitch of the grooves, is the same for all sample rotors.

Sealing Line Length And Blow Hole Area

As mentioned above, when the rotors rotate, a leading section of sealing line appears and as rotation continues, the line moves parallel to the z-axis, and eventually disappears as seen in Fig.3. Therefore, sealing line length varies as the rotors rotate.

Fig.7 shows interlobe sealing line lengths for the sample rotors characterized in Table 2. The interlobe leakage path area is obtained as the product of the sealing line length and the clearance. Blow hole areas also vary as the rotors rotate, because they appear or disappear due to the parallel movement along the z-axis. There are two blow holes for each groove. A leading hole exists toward the preceding adjacent groove, and a trailing hole exists toward following adjacent groove. The area of both blow holes is equal. Fig.8 shows the leading blow hole area for each sample rotor. It is clear from this figere that the maximum blow hole area increases with decreasing wrap angle.

Besides the above leakage paths, lobe tip clearances and lobe end clearances are also considered in the simulation program.

Discharge Port

Fig.9 shows a schematic view of the discharge port. It is comprised of a radial port component and an axial port component. The area of the axial port component is shown in Fig.10 for the sample rotors, as a function of rotor turning angle. The built-in pressure ratio of these sample rotors is fixed at 8. The radial port area is negligible when the built-in pressure ratio is large, as it is for these sample rotors. As seen in Fig.10, it is evident that the port opening area increases as the wrap angle increases.

ANALYTICAL MODEL OF COMPRESSION CYCLE

Fundamental Equations

Since a screw compressor is a positive displacement machine, the working space can be modeled by a chamber composed of a piston and a cylinder, connected to inlet and discharge valves, leakage paths, and oil-injection nozzles, as shown in Fig.11.

The following factors are taken into account in the model.

(1) Volume change due to rotor rotation.
(2) Mass and enthalpy flows of gas, entering or leaving the space through the inlet port, discharge port and leakage paths.
(3) Mass and enthalpy flows of oil, entering or leaving the space through the injection nozzle, inlet port, discharge port, and leakage paths.
(4) Heat exchange between gas and oil.

In order to simplify the calculations, the following assumptions are made.

(1) Gas and oil never change phase.
(2) Gas and oil temperatures are homogeneous throughout the working space at any instant.

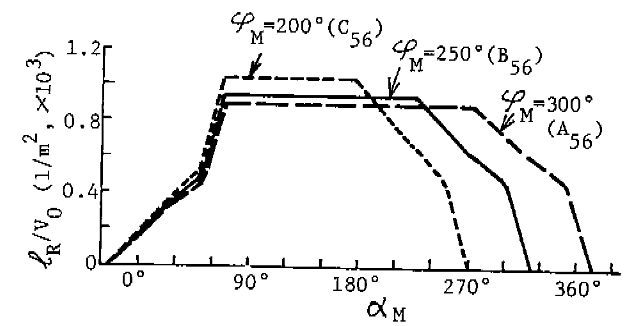

Fig.7 Interlobe Sealing Line Length

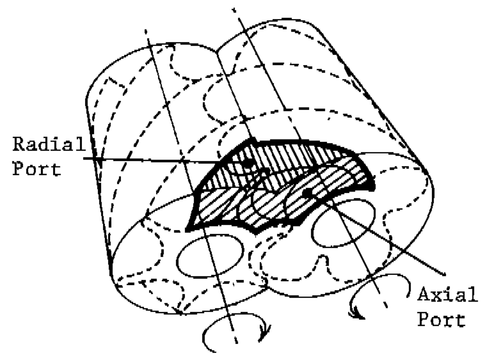

Fig.9 Discharge Port

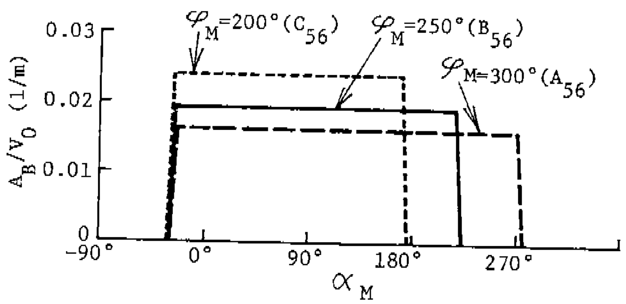

Fig.8 Blow Hole Area

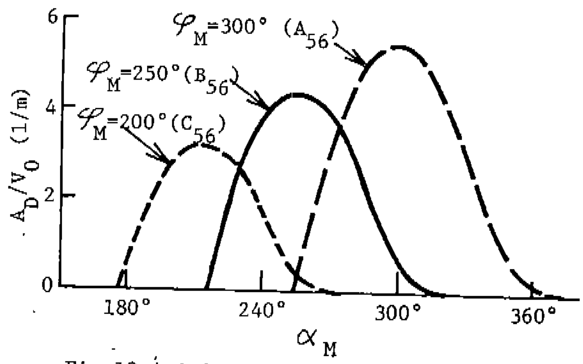

Fig.10 Axial Discharge Port Area

(3) Pressure is homogeneous throughout the working space at any instant.
(4) The working gas is an ideal gas.
(5) Oil is an incompressible fluid.
(6) Heat exchanged between gas and oil is in proportion to the temperature difference between gas and oil.
Then, the following fundamental equations are obtained.

$$\frac{dT_g}{dt} = -\frac{(\kappa-1)T_g}{V_g}\left(\frac{dV}{dt} - \frac{p_i}{p}q_{\ell i} + q_{\ell o}\right) + \frac{1}{M_g}(\kappa T_{gi} - T_g)m_{gi} - \frac{\kappa-1}{M_g}T_g m_{go} - \frac{hS}{C_v M_g}(T_g - T_\ell) \quad (9)$$

$$\frac{dp}{dt} = \frac{1}{V_g}\left[\left\{-\kappa p\left(\frac{dv}{dt} + q_{\ell o}\right) + (\kappa p_i - p_i + p)q_{\ell i} + \kappa\frac{T_{gi}}{T_g}\frac{p}{M_g}m_{gi} - \kappa\frac{p}{M_g}m_{go} - \frac{phS}{M_g C_v}\left(1 - \frac{T_\ell}{T_g}\right)\right\}\right] \quad (10)$$

$$\frac{dT_\ell}{dt} = (T_{\ell i} - T_\ell)\frac{1}{M_\ell}m_{\ell i} + \frac{T_\ell hS}{M_\ell C_\ell}(T_g - T_\ell) \quad (11)$$

$$\frac{dM_g}{dt} = m_{gi} - m_{go} \quad (12)$$

$$\frac{dM_\ell}{dt} = m_{\ell i} - m_{\ell o} \quad (13)$$

Using the above equations, changing in state in the working space can be calculated in a step-by-step procedure.

Discharge Process

All the equations obtained above are also used for the discharge process. For the sake of simplicity, the outlet chamber pressure is assumed to be constant.

Suction Process

Since pressure and temperature fluctuations in the suction process are genarally small, the following quantities are assumed to be constant during this process.
(1) Inlet velocities of gas and oil
(2) Temperatures of gas and oil
(3) Pressure drop across the inlet port.
(4) Heat flow from gas to oil (or from oil to gas).
Furthermore, it is also assumed that the inlet velocities of gas and oil are equal. Using the equation for energy balance and the law of mass conservation under the above assumptions, the states of gas and oil at the end of the suction process can be obtained analytically. The results are omitted for the sake of brevity.

Leakage Flow Rate

Leakage is a major concern in screw compressors.

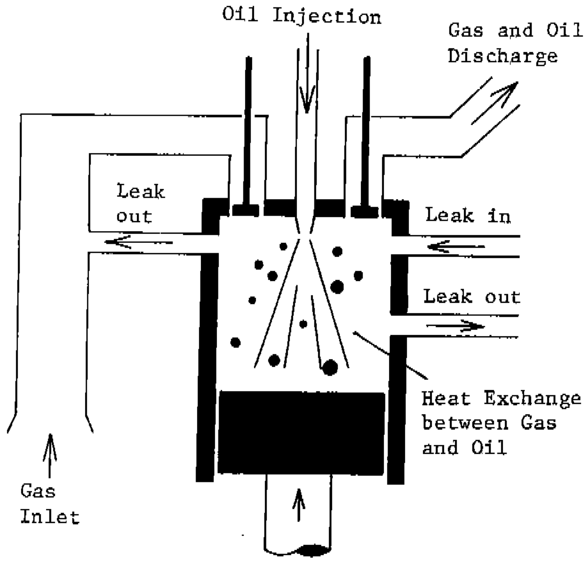

Fig.11 Working Space Model

However, it is difficult to estimate exact leakage values, especially in oil-injected screw compressors.
The following simplifying assumptions were made to calculate the leakage.
(1) Except at the lobe tip clearance, leakage gas and oil are uniformly mixed and flow isolated from heat exchange with their surroundings while maintaining thermal equilibrium. Flow rate is obtained using the well known equation of flow through a convergent nozzle, modifying the adiabatic exponent and gas constant as follows:

$$\beta = \frac{C_p + \phi C_\ell}{C_v + \phi C_\ell} \quad (14)$$

and,

$$R_m = \frac{1}{1+\phi}R \quad (15)$$

The effect of oil viscosity is added to the flow rate by adjusting the flow coefficient which must be determined empirically.
(2) At the lobe tip, the clearance fills with oil due to the action of centrifugal force and the oil leakage flow is in the single phase. Then the leakage flow rate can be calculated using the equation of incompressible viscous flow through a narrow channel developed, for example, by Ichikawa [3]

Definition Of Efficiencies

Volumetric efficiency η_v is defined by the following expression:

$$V = \frac{V_{gA}}{V_0} \quad (16)$$

where,

$$V_{gA}=\frac{M_{gA}RT_A}{p_A} \tag{17}$$

Adiabatic efficiency η_{ad} is:

$$\eta_{ad}=\frac{A_{th}}{A_i} \tag{18}$$

where,

$$A_{th}=\frac{\kappa}{\kappa-1}p_A V_{gA}\left\{\left(\frac{p_D}{p_A}\right)^{\frac{\kappa-1}{\kappa}}-1\right\} \tag{19}$$

In this paper, mechanical loss is not considered in η_{ad}.

OUTLINE OF COMPUTER PROGRAM

Fig.12 shows the flow diagram of the computer program. Input and output are listed in Table 3 and Table 4, respectively.
In the steady state, all changes in grooves are related to rotor turning, and the state in a groove varies as a function of the rotor turning angle. Therefore, when the change in state of one groove is calculated, the states in all grooves are known.
Step-by-step calculation starts from the end of the suction process. In order to calculate a leakage flow rate, the state of the groove beyond the leakage path must be known, although it is not determined at the beginning of the calculations. Therefore, the initial state in the groove is calculated under the condition of no leakage. Subsequently, the leakage flow is calculated and the state is corrected with the Runge-Kutta procedure. This calculation is iterated until the system converges.
Finally, volumetric efficiency, adiabatic efficiency, etc. are calculated.

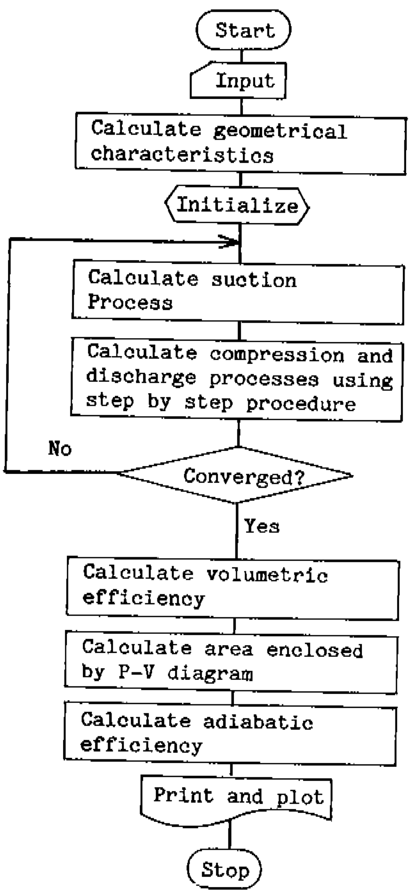

Fig.12 Flow Diagram

NUMERICAL EXAMPLES OF THE SIMULATION

Calculating Conditions

In this paper, perfomance is calculated for oil-injected air compressors fitted with the sample

Table 3 Input Data

a. Compressor Data
(1) Profile pattern
(2) Combination of teeth numbers
(3) Detail proportion of the profile
(4) Clearance of leakage path
(5) Built-in volume ratio
b.Operating conditions
(1) Inlet temperature
(2) Inlet pressure of gas
(3) Discharge pressure of gas
(4) Rotor rotation speed
(5) Supplied oil flow rate
(6) Supplied oil temperature
(7) Physical properties of gas and oil

Table 4 Output Data

a.Printer
(1) Volumetric efficiency
(2) Adiabatic efficiency
(3) Indicated power
(4) State of gas and oil in a groove as a table function of rotor turning angle
b.Plotter
(1)P-V diagram

Table 5 Values Used for Calculation

ε_R	0.03mm
ε_C	0.03mm
ε_D	0.03mm
π_i	8
α_J	100°
Working gas	Air
N	4000rpm
Inlet gas temperature	293.K
Supplied oil temperature	323.K
Supplied oil quantity	35ℓ/min
p_D	0.93MPa
p_A	0.10MPa

rotors descrived in Table 2. The parameters listed in Table 5 are used in the calculations.

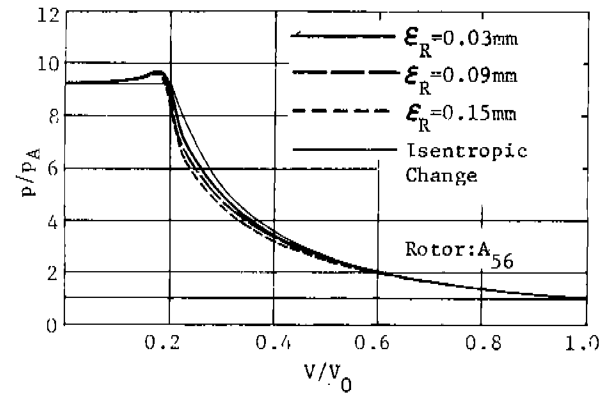

Fig.14 Effect of Interlobe Clearance on P-V Diagram Profile

<u>Effect Of Internal Leakage On Performance</u>

Fig.13 shows leakage flow rates through the leakage paths as functions of the rotor turning angle. All leakage rates are divided by the mass of theoretical intake gas. The largest leakage occurs through interlobe clearance as can be seen in Fig.13. This is due to the high pressure ratio across the leakage path.

The rate of leakage flow due to interlobe clearance is more or less flat in the region of the rotor turning angle between 100 and 180 degrees, where the pressure is probably rising due to compression. This is thought to be caused by the increasing mass fraction of oil in the working space, due to oil-injection.

Fig.14 shows the effect of interlobe clearance on the P-V relationship for the A_{56} rotor. It is observed that the pressure in the compression process decreases as the interlobe clearance increases. This is because of the decreasing mass in the working space.

Fig.15 shows the efficiencies and indicated torque on the driving shaft. As seen in the figure, indicated torque, and the volumetric and adiabatic efficiencies decrease as the interlobe clearance increases. In addition, the efficiencies fall at lower rotating speeds, because the amount of leakage mass increases in proportion to the time required for the compression cycle. These relationships are well known experimentaly.

The blow hole area is inherent in the contour of the rotor and can not be changed independently of the other characteristics, but computer simulation enables different values to be used. Fig.16 shows the effects of varying blow hole area on the P-V relationship for the A_{56} rotors. The pressure in

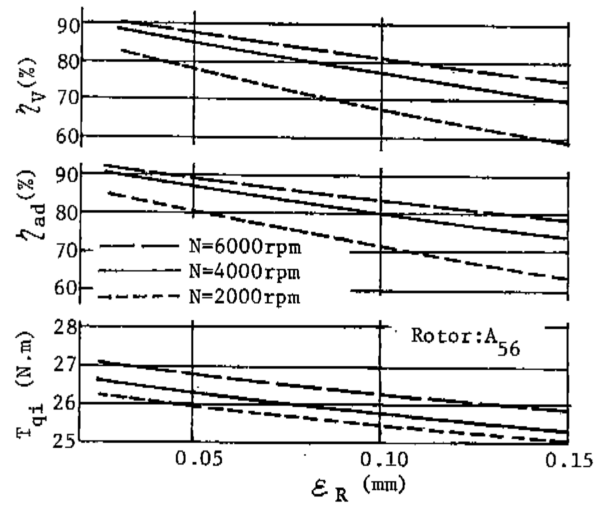

Fig.15 Effect of Interlobe Clearance on Performance

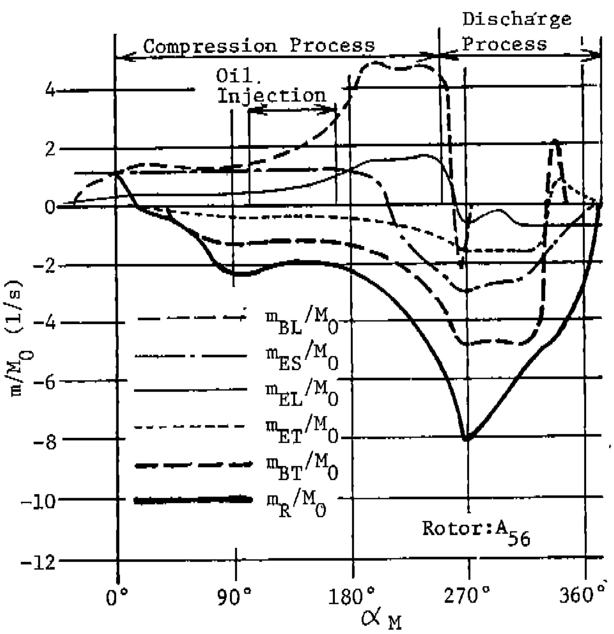

Fig 13 Leakage Flow Rate of Gas

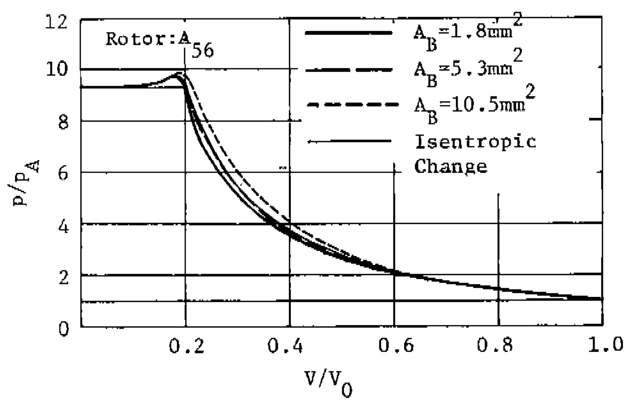

Fig.16 Effect of Blow Hole Area on P-V Diagram Profile

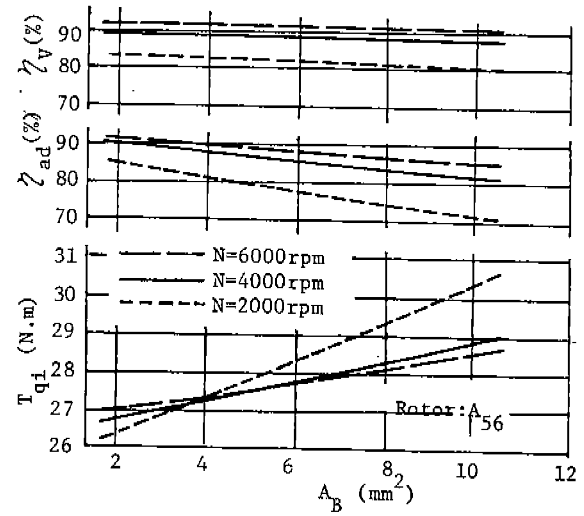

Fig.17 Effect of Blow Hole Area on Performance

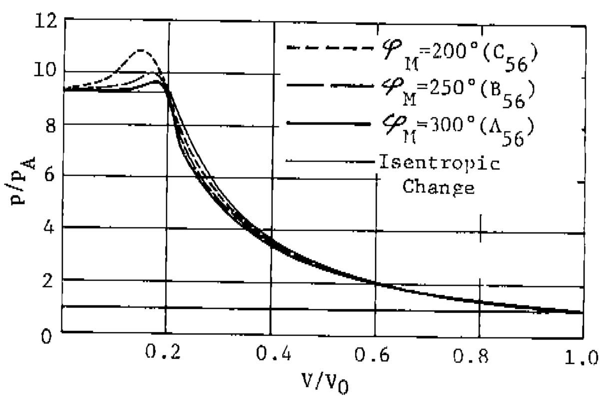

Fig.18 Effect of Wrap Angle on P-V Diagram Profile

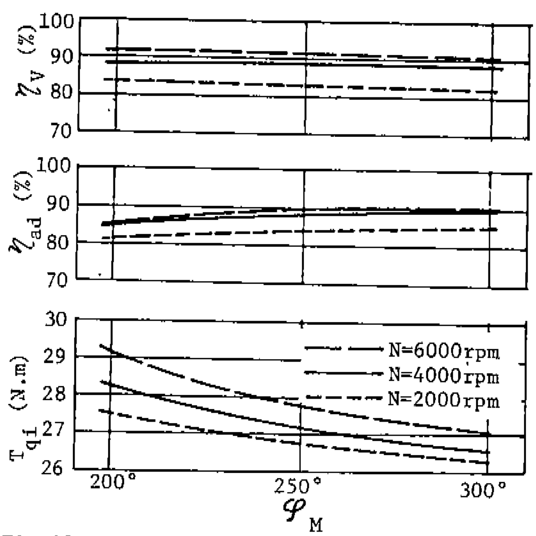

Fig.19 Effect of Wrap Angle on Performance

the compression process increases as the blow hole area is enlarged.

As seen in Fig.13, m_{BL} which refers to the leakage entering from the preceding adjacent groove, is larger than m_{BT} which refers to the leakage leaving to the following adjacent groove, over almost the entire region of the compression process. Consequently, when the blow holes are enlarged, the circulating mass increases and causes higher pressure in the working chamber.

The efficiencies and indicated torque are shown in Fig.17, as functions of blow hole area. It can be seen that the effect of blow hole area on the volumetric efficiency is rather small, but it exerts a significant influence on the adiabatic efficiency. In addition, it can also be seen that when the blow hole area is small, the indicated torque increases with increasing rotor speed, while this tendency is reversed for larger blow hole areas.

Effect Of Wrap Angle On Performance

Fig 18 shows the effect of wrap angle on the P-V relationship. It is noticed that the P-V diagram is slightly expanded in the case of a smaller wrap angle. As seen in Fig.8 and Fig.10, when the wrap angle becomes large, the blow hole expands and the dicharge port contracts. Therefore, the internal leakage circulating in the grooves increases and flow resistance across the discharge port becomes higher.

Fig.19 shows the effect of wrap angle on the efficiencies and the indicated torque. It is evident that the indicated torque increases as the wrap angle becomes smaller, corresponding to the increases in leakage loss and discharge loss as described above. Volumetric efficiency does not varies as the wrap angle changes. However, the adiabatic efficiency decreases as the wrap angle decreases.

SUMMARY AND CONCLUSIONS

A simulation model has been developed for evaluating the performance of screw compressors. The model allows wrap angle and blow hole sizes to be varied, thus facilitating analysis of screw compressors. Volume curves have been calculated from sealing lines, using the principle of virtual work. Flow resistance at inlet and discharge ports, internal leakage, and sealing and cooling effects of oil have been considered in the model. The efficacy of the model for analyzing screw compressor performance has been demonstrated by numerical examples.

REFERENCES

[1] Fujiwara, M., Mori, H. and Suwama, T., Proceedings of the 1974 Purdue Compressor Technology Conference, p.186-p.189

[2] Wilson, W. A. and Crocker, J. W., Mechanical Engineering, June(1946) p.514-p.518

[3] Ichikawa, T., Transactions of Jpn Soc. Mech. Eng. 18-73(1952) p.17